STM Study of Molecule Double-Rows in Mixed Self-Assembled Monolayers of Alkanethiols

ARTICLE *in* LANGMUIR · MARCH 2010

Impact Factor: 4.46 · DOI: 10.1021/la9044754 · Source: PubMed

Langmuir
Article
pubs.acs.org/Langmuir

STM Study of Molecule Double-Rows in Mixed Self-Assembled Monolayers of Alkanethiols

Gengzhao Xu,*,† D. Phillip Woodruff,‡ Neil Bennett,† Martin Elliott,† and J. Emyr Macdonald†

†School of Physics and Astronomy, Cardiff University, Cardiff CF24 3AA, U.K., and ‡Department of Physics, University of Warwick, Coventry CV4 7AL, U.K.

Received November 26, 2009. Revised Manuscript Received February 14, 2010

Using scanning tunnelling microscopy (STM), we have studied mixed self-assembled monolayers of linear alkanethiol molecules. Nonanedithiol (C9S2), nonanethiol (C9S), decanethiol (C10S), and dodecanethiol (C12S) were inserted into a self-assembled octanethiol (C8S) host matrix monolayer on an Au(111) surface using a two-step method. Quasi-one-dimensional double-row structures were found in the ordered, close-packed domains of the C8S matrix for each mixed monolayer system. These close-packed domains coexist with ordered striped phase domains (for C9S and C10S) or with a disordered phase (for C9S2 and C12S). Results from high-resolution images suggest that the double-rows are composed of inserted non-nearest-neighbor substitutional molecules, the ordering of which may be a result of locally induced surface stress.

1. Introduction

Self-assembled supramolecular structures of organic molecules on flat solid surfaces have been extensively studied in recent years. Structures result from a subtle balance of molecule−molecule interactions and molecule−substrate interactions.[1] Since it avoids the challenging task of the production of templates, this approach has attracted great interest in fabricating artificial structures on the nanometer scale. Besides extended two-dimensional layers, quasi one-dimensional molecular chains have also been observed. Directional intermolecular interactions such as hydrogen bonds,[2−6] substrate-mediated interactions,[7,8] or polymerization reactions on the surface initiated by a voltage pulse of an STM tip[9] drive the formation of molecular chain structures.

On the other hand, self-assembled monolayers (SAMs) of thiol-based molecules are often used to modify or control the properties of a metal surface.[10,11] Applications range from wetting control,[12,13] corrosion inhibition,[14] protein adsorption,[15] lateral patterning,[16] to molecular electronics.[17] Mixed SAMs that consist of more than one component are widely used because they provide additional flexibility.[18] Linear alkanethiols are often used as the host matrix material in mixed SAMs due to their closely packed, well-ordered arrangements[10] and large HOMO−LUMO energy gap (~8 eV).[19] The main features of the ordering of these deprotonated *n*-alkanethiol (alkylthiolate) SAMs have been established through a series of experiments using X-ray diffraction (XRD),[20] He atom scattering,[21] and scanning tunnelling microscopy (STM).[10] In particular, at a nominal coverage of 0.33 ML (i.e., one third the packing density of Au atoms in a single Au(111) layer), the basic ordering is on a $(\sqrt{3} \times \sqrt{3})$R30° mesh. For the longer alkane chains a $c(4 \times 2)$ superlattice of this basic structure generally dominates, whose true primitive surface mesh is $(3 \times 2\sqrt{3})$rect., containing four (inequivalent) thiolate species. In this high-coverage phase the molecules "stand up", with the alkane chain axis tilted by ~30° from the surface normal, bringing the chains into closer contact and enhancing the intermolecular van der Waals interaction. However, the details of the structure of the thiol−gold interface remain controversial. Even for the shortest alkane chains and the simplest $(\sqrt{3} \times \sqrt{3})$R30° ordered phase the local S-headgroup geometry remains a subject of debate, although it now seems to be established that the S atom occupies a local atop site relative to a surface Au atom[22,23] and that the thiolate is bonded to Au adatoms,[24,25] For the $(3 \times 2\sqrt{3})$rect.

*Corresponding author. Telephone: +44-(0)29 208 70162. Fax: +44-(0)29 208 74056. E-mail: xug2@cf.ac.uk.

(1) Kuhnle, A. Curr. *Opin. Colloid Interface Sci.* **2009**, *14*, 157.
(2) Bohringer, M.; Morgenstern, K.; Schneider, W. D.; Berndt, R.; Mauri, F.; De Vita, A.; Car, R. *Phys. Rev. Lett.* **1999**, *83*, 324.
(3) Weckesser, J.; De Vita, A.; Barth, J. V.; Cai, C.; Kern, K. *Phys. Rev. Lett.* **2001**, *87*, 096101.
(4) Barth, J. V.; Weckesser, J.; Cai, C.; Gunter, P.; Burgi, L.; Jeandupeux, O.; Kern, K. *Angew. Chem., Int. Ed.* **2000**, *39*, 1230.
(5) Ecija, D.; Otero, R.; Sanchez, L.; Gallego, J. M.; Wang, Y.; Alcami, M.; Martin, F.; Martin, N.; Miranda, R. *Angew. Chem., Int. Ed.* **2007**, *46*, 7874.
(6) Yokoyama, T.; Yokoyama, S.; Kamikado, T.; Okuno, Y.; Mashiko, S. *Nature* **2001**, *413*, 619.
(7) Lukas, S.; Witte, G.; Woll, Ch. *Phys. Rev. Lett.* **2002**, *88*, 028301.
(8) Kuhnle, A.; Molina, L. M.; Linderoth, T. R.; Hammer, B.; Besenbacher, F. *Phys. Rev. Lett.* **2004**, *93*, 086101.
(9) Okawa, Y.; Aono, M. *Nature* **2001**, *409*, 683.
(10) Poirier, G. E. *Chem. Rev.* **1997**, *97*, 1117.
(11) Schreiber, F. *Prog. Surf. Sci.* **2000**, *65*, 151.
(12) Bain, C. D.; Whitesides, G. M. *J. Am. Chem. Soc.* **1988**, *110*, 6560.
(13) Morgenthaler, S.; Lee, S.; Zurcher, S.; Spencer, N. D. *Langmuir* **2003**, *19*, 10459.
(14) Scherer, J.; Vogt, M. R.; Magnussen, O. M.; Behm, R. J. *Langmuir* **1997**, *13*, 7045.
(15) Song, S.; Clark, R. A.; Bowden, E. F. *J. Phys. Chem.* **1993**, *97*, 6564.
(16) Smith, R. K.; Lewis, P. A.; Weiss, P. S. *Prog. Surf. Sci.* **2004**, *75*, 1.
(17) Chen, F.; Hihath, J.; Huang, Z.; Li, X.; Tao, N. J. *Annu. Rev. Phys. Chem.* **2007**, *58*, 535.
(18) Lussem, B.; Muller-Meskamp, L.; Karthauser, S.; Waser, R.; Homberger, M.; Simon, U. *Langmuir* **2006**, *22*, 3021.
(19) Wang, W.; Lee, T.; Reed, M. A. *Phys. Rev. B* **2003**, *68*, 035416.
(20) Fenter, P.; Eisenberger, P.; Liang, K. S. *Phys. Rev. Lett.* **1993**, *70*, 2447.
(21) Camillone, N., III; Chidsey, C. E. D.; Liu, G.; Scoles, G. *J. Chem. Phys.* **1993**, *98*, 3503.
(22) Kondoh, H.; Iwasaki, M.; Shimada, T.; Amemiya, K.; Yokohama, T.; Ohta, T.; Shimomura, M.; Kono, K. *Phys. Rev. Lett.* **2003**, *90*, 066102.
(23) Roper, M. G.; Skegg, M. P.; Fisher, C. J.; Lee, J. J.; Dhanak, V. R.; Woodruff, D. P.; Jones, R. G. *Chem. Phys. Lett.* **2004**, *389*, 87.
(24) Maksymovych, P.; Sorescu, D. S.; Yates, J. T., Jr. *Phys. Rev. Lett.* **2006**, *97*, 146103.
(25) Yu, M.; Bovet, N.; Satterley, C. J.; Bengió, S.; Lovelock, K. R. J.; Milligan, P. K.; Jones, R. G.; Woodruff, D. P.; Dhanak, V. *Phys. Rev. Lett.* **2006**, *97*, 166102.

phase of the longer alkane chain species some general symmetry constraints for the structure have been defined by X-ray[20] and low energy electron diffraction,[26] but the exact structure remains unresolved. These symmetry constraints define the relative coordinates of pairs of thiolate species within the unit mesh, but the original idea that these "pairs" were only 2.2 Å apart and formed true chemical dimers[20] is no longer generally accepted. Moreover, many metastable adsorption phases of alkanethiols on Au(111) surface were also found at lower coverage and various temperatures.[27]

In this paper, we report an STM investigation of mixed SAMs of two closely related linear alkanethiol molecules on an Au(111) surface. In previous studies, similar mixed SAMs have been prepared from a single solution of the two component molecules and have led to monolayers that are either homogeneously mixed or are segregated into different domains, depending on the difference in chain length.[18,28] By contrast, in our model systems, the SAMs were prepared via a two-step method, in which a preassembled, closely packed SAM of octanethiol molecules is dipped in a second step into a solution of a second kind of alkanethiol molecule with a longer alkyl chain. In this second step, some host matrix molecules are substituted by the longer molecule. As a result, well-ordered domains with the $(\sqrt{3} \times \sqrt{3})R30°$ lattice of the host matrix coexisting with striped domains (or disordered domains in some cases) appeared on the surface after the second deposition step. Within the ordered domains, self-assembled quasi-one-dimensional double-rows of protrusions were also found, that are attributed to inserted longer-chain thiols.

2. Experimental Details

Toluene, 1-octanethiol (C8S), 1-nonanethiol (C9S), 1,9-nonanedithiol (C9S2), 1-decanethiol (C10S), and 1-dodecanethiol (C12S) were purchased from Sigma-Aldrich and used as received without any further purification. Au wire and mica slices were purchased from Goodfellow Cambridge Limited. Pt−Ir wires for STM tips (90%−10%) of 0.25 mm diameter were purchased from ChemPur.

Au(111) films were prepared by thermal evaporation of gold in ultrahigh vacuum (UHV) onto mica substrates which were kept at a temperature of 360−380 °C.[29] The base pressure was maintained lower than 3×10^{-9} mbar during the evaporation in order to form an atomically flat surface. After the sample was cooled down, it was transferred from the UHV system to a N_2 glovebox.

In the N_2 glovebox, mixed SAMs were prepared at room temperature. Au/mica samples were first immersed in a 5×10^{-5} M toluene solution of C8S for 2−3 h followed by a rinse in pure toluene for 5−10 s and drying in a N_2 flux. Then the sample was immersed in a toluene solution of the second alkanethiol (C9S, C9S2, C10S, or C12S) molecules at a concentration of 5×10^{-5} M for 3 min. Finally, the samples were rinsed in pure toluene and dried in flowing N_2 gas again. In the remainder of this paper, the deposition time and solution concentration refer to this second step.

The prepared surfaces were measured with a Veeco Multimode scanning probe microscope (SPM) in air. Mechanically cut Pt−Ir tips were used in the STM experiments and the specified bias was applied to the tip.

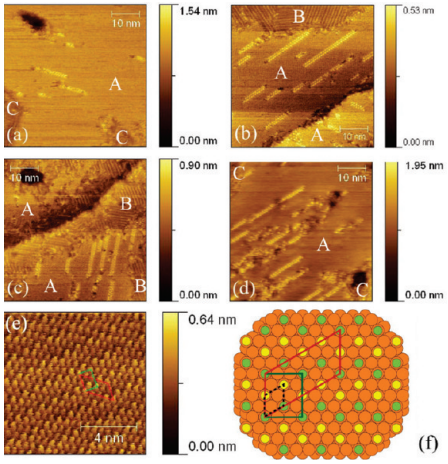

Figure 1. STM images of mixed SAMs on Au(111) surfaces. All images were taken under a tunneling condition of $V_b = -1$ V and $I_t = 200$ pA. Key: (a) C9S2 and C8S; (b) C9S and C8S; (c) C10S and C8S; (d) C12S and C8S. (e) A high-magnification image of an ordered, close-packed domain of the C8S host matrix on the sample of C9S2 and C8S. (f) Model of the commensuration between the alkanethiol SAM molecules, represented by the S headgroup atoms (small yellow and green circles), and the Au(111) surface atoms (larger orange circles). In parts a−d, ordered standing-up domains, ordered-striped domains, and disordered domains are labeled A, B, and C respectively. In part f, all S atoms are shown in identical atop sites but with two different color shading to represent some inequivalence; the inequivalence has been variously attributed to different alkane chain orientations, different sites, and the presence of bridging Au adatoms. In parts e and f, green lines and red lines represent the primitive $(3 \times 2\sqrt{3})$ rect. unit mesh and the $c(4 \times 2)$ superlattice of the basic $(\sqrt{3} \times \sqrt{3})R30°$ periodicity (shown by the dashed black lines). Within the primitive unit mesh there are four thiolate molecules comprising two pairs with the same relative locations within the pairs. The intermolecular spacing in the regular $(\sqrt{3} \times \sqrt{3})R30°$ structure is 0.499 nm.

3. Results and Discussion

Typical STM images of four different mixed SAMs, C9S2/C8S, C9S/C8S, C10S/C8S, and C12S/C8S on Au(111) surface are displayed in Figure 1, parts a−d. Images were acquired with a voltage bias of −1 V and a tunnelling current of 200 pA. On the samples of C9S2/C8S (Figure 1a) and C12S/C8S (Figure 1d), both well-ordered close-packed "standing-up" domains, as observed for pure C8S matrix monolayers, and disordered domains were observed. For the C9S/C8S (Figure 1b) and C10S/C8S (Figure 1c) samples, the ordered close-packed "standing-up" domains were observed to coexist with ordered striped domains, in which the molecules lie flat on the surface. The ordered standing-up domains, ordered-striped domains and disordered domains are labeled A, B, and C respectively in Figure 1, parts a−d. However, double rows of protrusions were found in the ordered, close-packed domains on all four samples. This behavior is quite different from that seen on samples prepared by a one-step method of coadsorption from a mixed solution,[30] in which phase segregation was observed if the chain length difference was greater than four carbons; otherwise the longer-chain alkanethiol molecules were randomly distributed in the matrix. Figure 1e is a higher-magnification image of a flat domain not containing the inserted double-rows, in which the host matrix molecules with a hexagonal $(\sqrt{3} \times \sqrt{3})R30°$ structure are clearly seen. A model of the commensuration between alkanethiol SAM and Au(111) surface is illustrated in Figure 1f.

(26) Chaudhuri, A.; Lerotholi, T. J.; Jackson, D. C.; Woodruff, D. P.; Jones, R. G. *Phys. Rev. B* **2009**, *79*, 195439.
(27) Poirier, G. E.; Fitts, W. P.; White, J. M. *Langmuir* **2001**, *17*, 1176.
(28) Kim, Y. K.; Koo, J. P.; Huh, C. J.; Ha, J. S.; Pi, U. H.; Choi, S. Y.; Kim, J. H. *Appl. Surf. Sci.* **2006**, *252*, 4951.
(29) Levlin, M.; Laakso, A.; Niemi, H. E. M.; Hautojarvi, P. *Appl. Surf. Sci.* **1997**, *115*, 31.
(30) Chen, S.; Li, L.; Boozer, C. L.; Jiang, S. *Langmuir* **2000**, *16*, 9287.

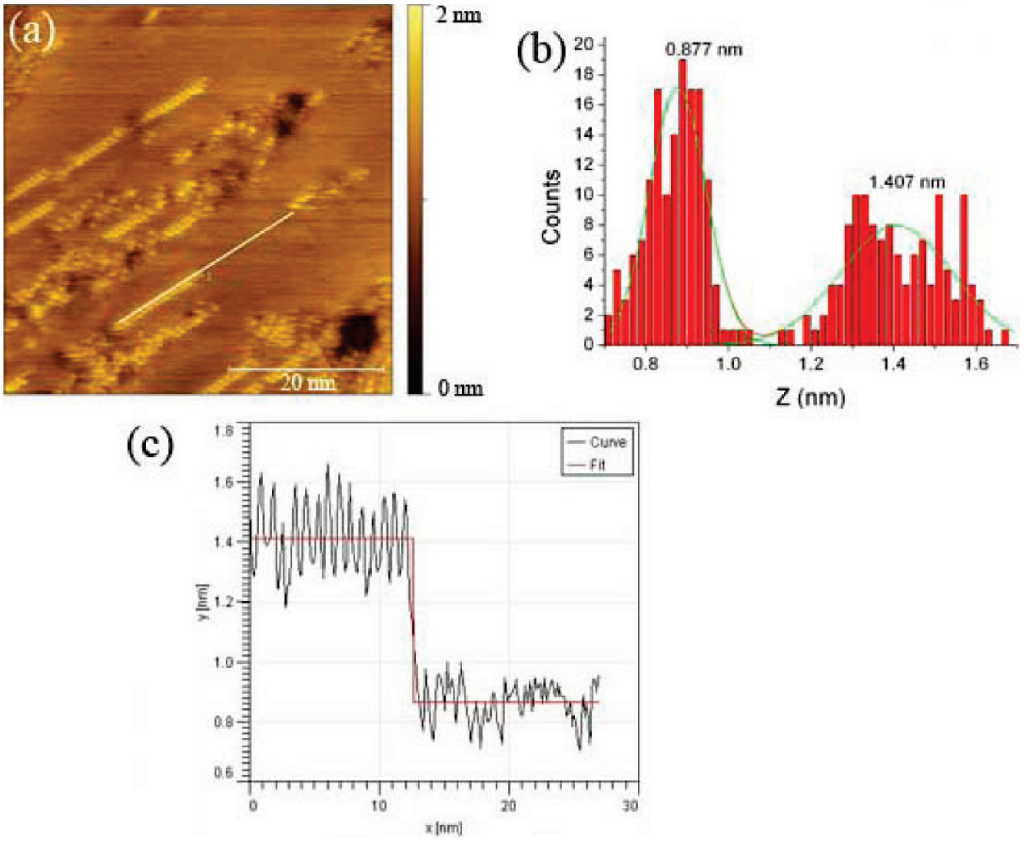

Figure 2. (a) STM image of mixed SAM of C12S and C8S. (b) Double-peak Gaussian fitting of the histogram of the profile along the white line in part a. (c) Step-function fitting of the same profile.

We used two methods to calculate the height difference between the double-rows and the ordered, close-packed domains of the host matrix on three samples of mixed SAMs which were composed of two kinds of alkane-monothiols (the samples of C9S/C8S, C10S/C8S, and C12S/C8S). An example of the measurements on the mixed SAM of C12S/C8S is illustrated in Figure 2. A profile was taken along the white line in Figure 2a. With the first method, a histogram of the height of the surface was determined. The height difference between the double-rows and the host matrix, was then determined from the amplitude of two Gaussian peaks fitted to this histogram, as shown in Figure 2b. With the other method, we directly fit the profile with a step function as shown in Figure 2c. The height differences obtained with these two methods, and the density and lengths of double-rows of three samples are displayed in Table 1. Then 22 double-rows were used to analyze the height difference of the C9S/C8S sample, which gave the most stable images as a result of the small height difference, 6 for C10S/C8S and 7 for C12S/C8S. The quoted errors represent the standard deviation of the height difference values. The height difference increases as the alkyl chain of the second alkanethiol gets longer. The length of the linear alkanethiol molecule, L, can be evaluated from the empirical equation[31,32]

$$L\ (\mathrm{nm}) = 0.25 + 0.127n$$

where n is the number of CH_2 groups. If we regard the molecules as linear, and take into account the 30° tilt angle of the alkyl chain, the height difference is predicted to be 0.11, 0.22, and 0.44 nm for the three samples, respectively. The measured height differences listed in Table 1 all agree with these predictions within the estimated precision. More exactly, of course, we should take account of the zigzag nature of the alkane chain. Specifically, in going from an even number of C atoms to an odd number, the direction of the terminal $C-CH_3$ bond in the chain is actually quite close to perpendicular to the surface (whereas that of molecules with an even number of C atoms is more-nearly parallel to the surface). The exact direction of these terminal $C-CH_3$ bonds depends on the azimuthal orientation of the plane of the alkane chain, but this general trend of a more-nearly perpendicular orientation for the $C-CH_3$ bond of the C9S molecule should be valid. The height increase for the C9S molecules in the C8S matrix should therefore be greater than the simple estimate of 0.11 nm given above; the experimental value given in Table 1 is, indeed, larger, but in view of the limited precision it is not clear that this result is significant.

While Table 1 appears to show rather good agreement between the expected and measured height differences for the protruding longer-chain thiolate molecules, we should note that some previous studies have cast doubt on whether this simple correlation should exist. Specifically, Bumm et al. have found that the height difference recorded in STM images from adjacent domains of C10S and C12S on Au(111) is only approximately half of the true value.[33] They rationalize this is terms of a model of tunnelling through the high-impedance molecules and adapt theoretical results from an earlier combined AFM/STM study[34] to support

(31) Motte, L.; Billoudet, F.; Pileni, M. P. *J. Phys. Chem.* **1995**, *99*, 16425.
(32) Bain, C. D.; Evall, J.; Whitesides, G. M. *J. Am. Chem. Soc.* **1989**, *111*, 7155.
(33) Bumm, L. A.; Arnold, J. J.; Dunbar, T. D.; Allara, D. L.; Weiss, P. S. *J. Phys. Chem. B* **1999**, *103*, 8122.
(34) Salmeron, M.; Neubauer, G.; Folch, A.; Tomitori, M.; Ogletree, D. F.; Sautet, P. *Langmuir* **1993**, *9*, 3600.

Table 1. Statistical Results for the Protruding Double-Rows

	height difference (double-peak Gaussian fitting) (nm)	height difference (step fitting) (nm)	number density of the double-rows (μm^{-2})	length of the double-rows (repeated units)
C8S/C9S	0.124 ± 0.038	0.118 ± 0.029	1996 ± 335	11 ± 7
C8S/C10S	0.213 ± 0.042	0.166 ± 0.043	682 ± 192	8.5 ± 6
C8S/C12S	0.38 ± 0.13	0.40 ± 0.13	443 ± 124	7 ± 3
C8S/toluene			125 ± 65	

their results. It is unclear why our results are at variance with this finding. The tunnelling currents we have used (200 pA) significantly exceed that (10 pA) used in the earlier study, but the theoretical treatment presented by Bumm et al. would appear to be equally applicable to our higher currents, at least for the C8S, C9S, and C10S molecules.

Table 1 also shows that the number density and the mean length of double rows decrease when the inserted molecules get longer. This indicates that the inserted molecules are more likely to be mixed into the well-ordered host matrix when their chain-length difference is smaller and otherwise they tend to segregate into different domains, an effect that has been reproduced in a Monte Carlo (MC) calculation.[35]

On the sample of C9S2/C8S, double-rows structures were also found in ordered-domains indicating that the inserted C9S2 molecules were standing up on the surface. No evidence was seen within these ordered "standing-up" regions of the matrix molecules for C9S2 molecules lying down on the surface despite the presence of thiol groups at each end: the observed structures are very similar to those observed in for the monothiol equivalents.

The question arises whether the STM images in Figure 1 represent the equilibrium structure or whether they are instantaneous arrangements well away from equilibrium. In order to address this issue, solution concentration and immersion time were varied in the second step of deposition. At a concentration of 5×10^{-5} M, double-rows were obtained after a deposition time ranging from 30 s to 30 min. At lower concentration, such as 5×10^{-7} M or 5×10^{-8} M, no double-rows were observed at all after deposition in the second step for 30 min. At a concentration of 5×10^{-6} M, double-rows were found in only one ordered domain among all the 17 ordered domains we investigated after a deposition time of 30 min. These measurements indicate that the double-row structures are formed during the second step of deposition and that these structures represent either a long-lived metastable state or a state close to thermal equilibrium.

A high-resolution image of the mixed SAM of C9S/C8S is presented in Figure 3a and shows clearly a double-row of bright protrusions associated with the intercalated C9S molecules, aligned along the direction 30° away from the molecular rows of the host matrix (that is to say, along the $[1\bar{1}0]$ direction of the Au(111) surface). Superimposed on part of this image is a grid drawn such the intersections of the lines are located above the protrusions associated with the C8S matrix molecules. This shows rather clearly that the centers of the somewhat elongated bright protrusions associated with the C9S molecules are located on the same mesh points as those of the C8S molecules. The simplest interpretation of this registry is thus that the C9S molecules occupy substitutional sites in the C8S matrix. Figure 3b shows a model based on this idea in which the interface structure is assumed to be based on the Au-adatom-dithiolate model.[24] The orange circles represent Au surface atoms, the red circles Au adatoms, the yellow circles S headgroup atoms of the C8S species and the large white circles S headgroup atoms of the C9S molecules. Of course, the STM does not image the S headgroup atoms, but rather the terminal methyl groups, as is clear from the correspondence of the height difference measured and predicted for the longer-chain intercalated molecules. However, if all the molecules have the same tilt direction, all the terminal methyl groups of the C8S molecules will have the same relative lateral positions as their S headgroup atoms, but with some net lateral displacement. Strictly, we might expect the terminal methyl group of the intercalated C9S molecules to have a lateral offset relative to those of the C8S matrix molecules because of the longer associated (tilted) alkane chain, but as remarked above the direction of the terminal $C-CH_3$ bond in the C9S chain with an odd number of C atoms is actually quite close to perpendicular to the surface. As such, the relative lateral positions of the protrusions imaging in the STM should be quite close to those of the associated S headgroup atoms for the C8S/C9S mixed phase. Notice, too, that while Figure 3b is based on the Au-adatom-dithiolate model of the interface, an equally acceptable interpretation would be achieved by omitting the Au adatoms, leaving the S headgroup atoms in simple unreconstructed atop sites, or, indeed, by also removing 2/3 of the outermost layer Au atoms (those not bonded to a S atom) to leave the interface described by the Au-adatom-monothiolate model.[25] Notice that in the model of Figure 3b there are no vacant thiolate sites. It is not really possible to tell, from the STM image of Figure 3a, if the C8S molecules between the two C9S molecular rows are present or not, but this image certainly does suggest that all the C8S molecules within the adjacent rows outside the C9S double row are present.

While Figure 3b (or variants on it with respect to the local interface structure described above) provides a simple model of the structure seen in the STM image, it leaves many questions unanswered. One such question concerns the elongated appearance of the C9S-derived protrusions. Indeed, it is tempting to interpret these protrusions as due to two closely spaced separate molecules. The associated spacing could be attributed to a dimer with a (S−S) spacing of 2.2 Å, (as indicated by a line-scan of the image) as proposed in the early XRD study,[20] but there is now a very considerable body of spectroscopic evidence that such dimers do not occur in these high coverage phases. Moreover, with a van der Waals radius of ~2 Å for the methyl group, it is particularly difficult to see how the images could be interpreted in this way. A more reasonable explanation is that the elongation reflects the ability of the protruding methyl group of the longer-chain molecules to have a larger amplitude wagging vibration than those of the more constrained C8S matrix.

A second question concerning this model is how the intercalated rows of longer-chain molecules nucleate in the surface. In this regard, it is notable that the end of the double-row feature of Figure 3a coincides with the location of a large dark feature, most obviously interpreted as some kind of extended vacancy defect. Inspection of a large number of images reveals that (as also seen in Figure 1) defects of this kind are always seen either at one end or at both ends of these intercalated double rows.

(35) Chevade, A. V.; Zhou, J.; Zin, M. T.; Jiang, S. *Langmuir* **2001**, *17*, 7566.

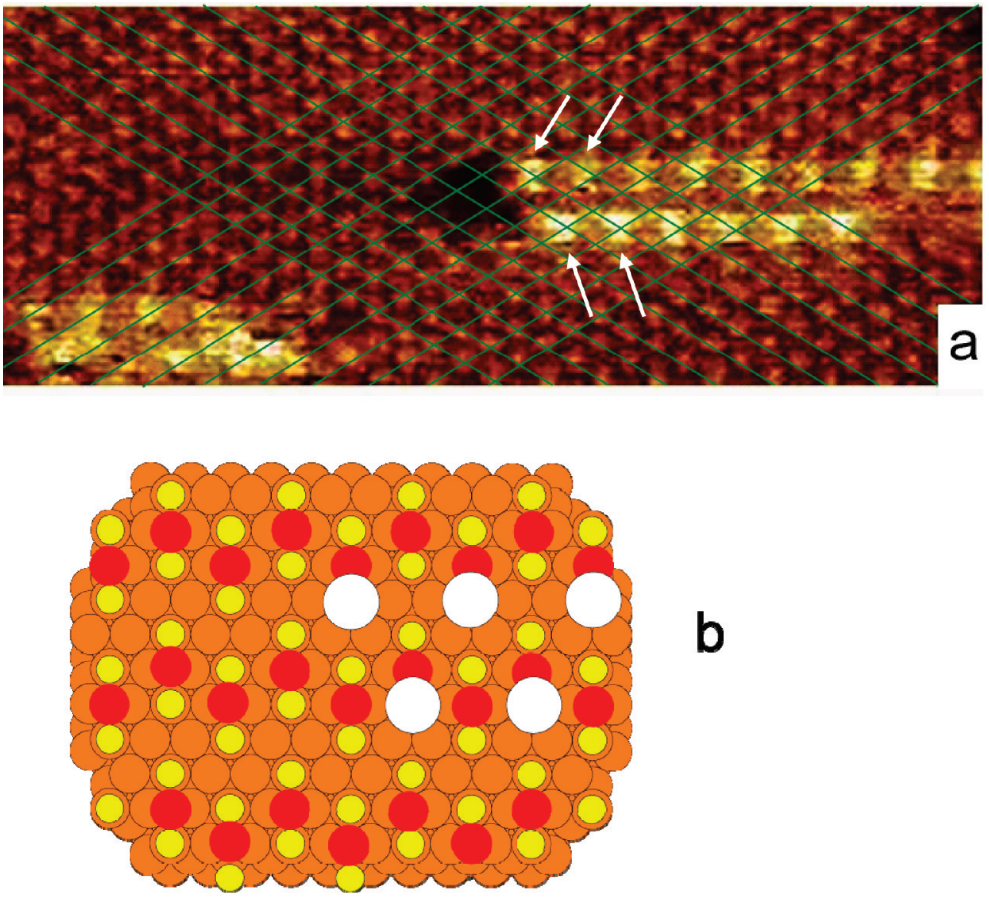

Figure 3. (a) High-resolution STM image of a double-row in the mixed SAM of C9S/C8S with a superimposed mesh such that the lines cross over the protrusions (as indicated by the arrows) of the C8S matrix SAM. (b) Model of the Au/thiolate interface of this structure based on the Au-adatom-dithiolate interface structure. Orange circles represent the Au surface atoms, red circles Au adatoms, yellow circles the S headgroup atoms of the C8S matrix and large white circles the S headgroup atoms of the C9S molecules.

This leaves as the most significant question as the remaining puzzle: why do the intercalated longer-chain molecules always form double-row structures? Conventionally, directional intermolecular interactions such as hydrogen bonds,[2−6] substrate-mediated interactions,[7,8] or polymerization reactions on the surface initiated by voltage pulse between an STM tip and the surface[9] were thought to be the main reasons for the formation of quasi-one-dimensional chain structures. However there are no additional functional groups on alkanethiol molecules that can generate directional intermolecular interactions between alkyl chains, and no voltage pulses were applied during the STM experiments. In Table 1, we can see that both the density and length of the double-rows reduce as the inserted molecules get longer.

One possible rationale for the double-row structure in the present case may be found in the known behavior of alkylthiolate SAMs on Au(111) as a function of alkane chain length. In particular, there are small but systematic differences in the apparent tilt angles, and in the azimuthal angle of tilt relative to the substrate, and hence also to the neighboring molecules, with increasing alkane chain length.[11] For both parameters some scatter in the measured angles makes it difficult to be sure whether this variation with chain length is smooth, although for the azimuthal angles, at least, this appears to be the case. One implication of this result is that inserting several near-neighbor C9S molecules into a C8S matrix SAM may be energetically unfavorable because of the different preferred tilt orientations determined by the intermolecular interactions of the molecules with the same chain length. This could account for the fact that, in the model of Figure 3b, the inserted C9S molecules do not occupy nearest-neighbor sites (neither within, not between, the Au−adatom dithiolate moieties). Moreover, one may surmise that even inserting a single longer-chain molecule into the surrounding matrix leads to some local compressive stress. Inserting a double row may therefore correspond to the maximum permitted stress perpendicular to these rows. Of course, parallel to the row there are many more than two inserted molecules, but in this direction there is some possibility of stress relief by strain into the vacancy defect at the end of the rows. One further observation that supports this general idea is that the energy cost and stress associated with the insertion will increase with increasing difference in the alkane chain length, an effect that could account for a reduction in both the number and length of the inserted double rows with increasing difference in the chain lengths.

In order to understand the influence of the solvent in the second deposition step, we investigated the effect of immersing a pure C8S-saturated sample in pure toluene for 3 min. STM images of this surface, comprising both ordered and disordered domains, are shown in Figure 4. In the middle of some ordered domains, missing rows were observed, as shown in Figure 4, parts a and b. A profile along the white line in Figure 4b is displayed in Figure 4c. The profile was drawn along the nearest neighbor molecule direction of the matrix lattice. Though the measured depth of the dark stripe is almost certainly less that the true height difference due to tip size effects, it is broadly consistent with there being no thiolate species in this region. The creation of these extended vacancy rows in the C8S matrix due to the effect of the

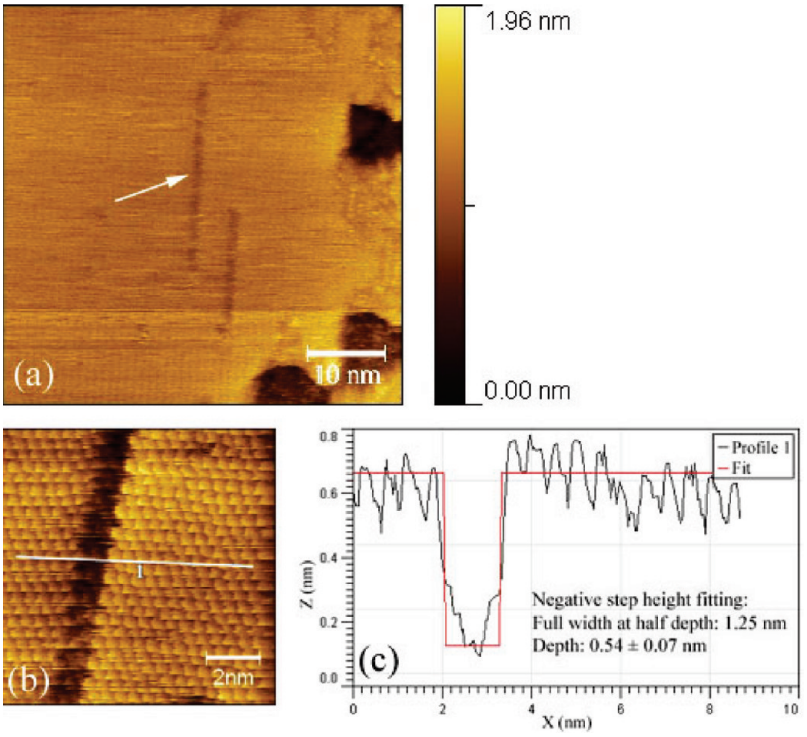

Figure 4. STM images of the sample which was immersed in pure toluene solvent for 3 min in the second deposition step. (a) Large-scale image, in which there are an ordered domain and a disordered domain (along the right side of the image). Missing-row defects are found inside the ordered domain, as indicated by the white arrow in this image. (b) High-resolution image of a missing row defect inside an ordered domain. (c) Line profile along the white line in part b.

toluene solvent is clearly suggestive that they relate to the formation of the double-rows of protruding alkanethiol molecules. The number density of these vacancy rows is around $125 \pm 65\ \mu m^{-2}$, a factor of > 10 greater than the density of double row protrusions for C8S/C9S SAMs (Table 1). Together with the dependence of the number density of double row protrusions on the chain length, as described in Table 1, it suggests that the formation of the double-row protrusions is caused by a dynamic substitution process. While the detailed mechanism may not be certain, it is plausible that the C8S molecules desorbed during the second immersion step are substituted by the longer alkanethiols at a rate related to the strain and concentration as discussed above. When immersed in pure toluene, the desorbed C8S molecules have a reasonably high probability of readsorbing rapidly, resulting in a smaller density of vacancy row structures being visible in STM images.

4. Conclusion

We have used STM to study mixed SAMs of C9S2/C8S, C9S/C8S, C10S/C8S, and C12S/C8S on Au(111) surfaces prepared by a two-step method. There were well-ordered and striped domains (or disordered domains) in the SAMs. Inserted double-rows of the longer molecules were found in the ordered domains of the C8S matrix on all the samples. We propose a possible driving force for this particular form of molecular insertion based on local strain as a result of differences in the preferred tilt and twist angles of the different chain length, partially relieved by the vacancy islands found at one end of all of the double molecular rows.

Acknowledgment. This work is supported by Engineering and Physical Sciences Research Council (Grant No. EP/D076072/1).